X-911-76-151
PREPRINT

SATELLITE-OBSERVED LATENT HEAT RELEASE IN A TROPICAL CYCLONE

ROBERT F. ADLER
EDWARD B. RODGERS

NOVEMBER 1976

GSFC — GODDARD SPACE FLIGHT CENTER —
GREENBELT, MARYLAND

X-911-76-151
Preprint

SATELLITE-OBSERVED LATENT HEAT RELEASE IN A TROPICAL CYCLONE

Robert F. Adler
Edward B. Rodgers

November 1976

GODDARD SPACE FLIGHT CENTER
Greenbelt, Maryland

Satellite-observed Latent Heat Release

in a Tropical Cyclone

Robert F. Adler

Edward B. Rodgers

Abstract

Data from the Nimbus 5 Electrically Scanning Microwave Radiometer (ESMR) are used to make calculations of the latent heat release (L. H. R.) and the distribution of rainfall rate in a tropical cyclone as it grows from a tropical disturbance to a typhoon. The results indicate that the latent heat release characteristics of tropical cyclones can be determined from the microwave data and that such observations are potentially useful in the monitoring of such storms. The L.H.R. (calculated over a circular area of 4° latitude radius) increases during the development and intensification of the storm from a magnitude of 2.7×10^{21} ergs s^{-1} (in the disturbance stage) to 8.8×10^{21} ergs s^{-1} (typhoon stag). The latter value corresponds to a mean rainfall rate of 2.0 mm hr^{-1}. Even during the disturbance stage, the L.H.R. increases significantly. It is also shown that the more intense the cyclone and the greater the L.H.R., the greater the percentage contribution of the larger rainfall rates to the L.H.R. In the disturbance stage the percentage contribution of rainfall rates ≥ 6 mm hr^{-1} is typically 8%; for the typhoon stage, the value is 38%. The distribution of rainfall rate as a function of radial distance from the center indicates that as the cyclone intensifies, the higher rainfall rates tend to concentrate toward the center of the circulation.

CONTENTS

ILLUSTRATIONS

1. Introduction

The release of latent heat through condensation and precipitation processes is essential to the development and maintenance of tropical cyclones. Tropical cyclone genesis appears to be related to Conditional Instability of the Second Kind (CISK) (Charney and Eliassen, 1964; Yanai, 1975). This energy source for the disturbance is dependent on the interaction of cumulus-scale convection and the synoptic-scale motion field. The large scale flow provides the moisture convergence necessary for the convection, and the heating due to condensation and precipitation maintains the large-scale disturbance.

The maintenance of mature tropical cyclones is also dependent on the energy provided by the latent heat release (L. H. R.). Energy budget studies by Palmen and Riehl (1957), Riehl and Malkus (1961), and Miller (1962) indicate that, for steady-state conditions, the outflow of energy is nearly equal to the L. H. R. The condensational heating produces the storm's warm core and temperature gradients, and thus the available potential energy necessary for conversion into kinetic energy.

The determination of the magnitude of the latent heat release in tropical cyclones is therefore important. Some previous estimates of the L.H.R. in a storm have been made using the moisture budget approach in which conventional and aircraft winds are used along with measurements of water vapor to calculate the moisture or latent heat flux across the boundary of the storm (or at a particular distance from the storm center). Assuming steady state, the precipitation inside the boundary is approximately equivalent to the boundary flux. This procedure has been used, for example, by Miller (1962), Palmen and Riehl (1957) and Riehl and Malkus (1961). Although radar observation of precipitation in tropical cyclones has added a great deal to our knowledge of the structure of the storms, no estimate of storm L. H. R. has been made with radar data.

The satellite microwave data used in this case study offer an opportunity to estimate the L. H. R. and distribution of rainfall rate in a tropical cyclone as

it develops from a disturbance into a typhoon. The satellite-based approach offers the only realistic way of making repeated calculations of L. H. R. in a storm over water.

2. Description of Data

The Nimbus 5 spacecraft, launched in December 1972, has a sun-synchronous orbit with local noon and midnight equator crossings. From a height of approximately 1100 km, successive orbits cross the equator with a separation of 27° longitude. The Electrically Scanning Microwave Radiometer (ESMR) on Nimbus 5 is a passive microwave instrument measuring emitted radiation in the 19.35 GHz (1.55 cm) region with a resolution of 25 km at nadir. The instrument is described in detail by Wilheit (1972). Over water, the microwave radiation emitted by the earth and atmosphere (expressed in terms of brightness temperature, T_B) is affected primarily by the state of the sea surface, and by atmospheric water vapor and atmospheric liquid water. Liquid water, in the form of drops of the size associated with rain, is the dominating factor in the variation of T_B over water.

Examples of Nimbus 5 ESMR images are discussed by Wilheit et.al. (1976). Allison et.al. (1974) use ESMR images along with visible and IR images to describe a number of tropical cyclones, including the storm used as a subject for the present study. These studies have shown that there is a qualitative relation between rainfall intensity over water and ESMR brightness temperature (T_B). Wilheit et. al. (1975) have quantified this relationship by using a theoretical model for microwave radiative transfer in the presence of rain. The model calculations are compared to satellite observations and calibrated radar measurements. A ground-based verification experiment was also carried out using an upward-looking microwave radiometer. The results of the comparisons were good, considering the inherent difficulties in measuring rain rate, and the problems of using radar-determined rain rates as "ground truth". Nearly

all the radar rainfall rates are within a factor of 2 or 2 mm hr^{-1} (whichever is larger) of the satellite-based estimate. Although this represents a large random error or difference, there is no obvious overall systematic bias. For the fifty points involved in the comparison, the mean rainfall rates derived from both the radar data and the satellite data differ by only approximately 5%. Therefore, even though there is a large random difference between the two estimates, the mean difference over a number of points is small.

3. Data Preparation and Method of Calculation

a. Brightness Temperature Adjustment - In order to calculate various rainfall rate parameters and the latent heat release for a storm, the ESMR brightness temperature data must be related to rainfall rate values and integrated over the appropriate area. In the present study, prior to the calculation being made, an adjustment of the ESMR T_B's is carried out, based on a statistical analysis of ESMR data by Kidder (1976). Using three months of Nimbus 5 ESMR data, he calculated mean brightness temperature as a function of scan position and time of observation (day or night) for 10° latitude by 10° longitude blocks over the Pacific Ocean. Over a three month period, the same geographic block was viewed at different angles by the instrument so that if there were no instrument bias, the mean T_B would be constant as a function of scan position. The statistics, however, show variations with scan position and between day and night observations. Most features in the statistics can be noted in all blocks, although amplitudes of the variations appear to be less at higher latitudes.

The combined statistics of the data in the 0-10°N strip are used as the basis for the adjustments in this study. This amounts to 4.5×10^5 points. Kidder's analysis was restricted to scan angles of less than 30°. At each scan position, the mean T_B for day passes is larger than that for night. There is also a general, weak increase of T_B with increasing scan angle. The causes of these variations are unknown, and the problem is under investigation. The

mean day-night difference is 4.0 K. The amplitude of the scan angle variation is 8.8 K at night and 6.6 K during the day. Although these magnitudes are small compared to the range of observed ESMR T_B in the tropics over oceans (~90 K), these variations might affect calculations of time changes in a storm observed with a number of orbits, including both day and night passes and centered at different scan angles.

An empirical scheme is devised to eliminate these variations. Nighttime, near nadir temperatures are arbitrarily decided to be correct and a base brightness temperature is chosen from that region. The observed T_B minus the base value as a function of day and night and scan angle is then used as the T_B adjustment. Within 30° of nadir, the mean absolute magnitude of the adjustment is 2.5 K, while the maximum value is 7.2 K.

b. Brightness Temperature-Rainfall Rate Relation - After the data are adjusted as described above, rainfall rate can be determined from the T_B - rainfall rate relation, which is a function of freezing level. For this case, a freezing level of 5 km is chosen. This is consistent with the temperature structure of Pacific Ocean cloud clusters and mature tropical cyclones. Pacific Ocean cloud clusters, from which the cyclones develop, have a freezing level at approximately 570 mb, or 4.7 km (Williams and Gray, 1973). Palmen and Newton (1969) show the temperature structure of a mature hurricane to have a freezing level of very close to 5.0 km, except near, and in the eye, where it is higher. In the present study, the same freezing level (5 km) is assumed for all satellite storm passes even though the height of the freezing level should increase slightly as the storm intensifies. Also, no spatial variation of freezing level is considered even for the mature storm when substantial horizontal temperature gradients are present.

The relation of rainfall rate to brightness temperature for a freezing level of 5 km is shown in Fig. 1. The curve intersects zero rain rate at $T_B = 177$ K. Above that value, increasing T_B indicates increasing rainfall rate. A T_B of

256 K is equivalent to 10 mm hr^{-1}. In the current study the highest T_B observed over the storm is 258 K. Temperatures above 256 K are assigned a rainfall rate of 10 mm hr^{-1}. Although this rain rate does not seem equal to the heavy rain observed in tropical systems, the satellite-based estimate is a mean for an area greater than 600 km^2.

c. Method of Calculation - The calculations are confined to a circular area of 4° latitude radius (444.4 km). For each satellite pass over the disturbance or storm, computations are made for two areas, the centers of which are determined in the following ways. First, a center of circulation is determined based on the microwave image and digital information, a concurrent infrared image and storm location information from the 1973 Annual Typhoon Report. The center of the circulation is usually well defined in the microwave data for mature systems. However, for disturbances and depressions a center of circulation is often not discernible in the data. For this reason, a second center of calculation is defined on the point of maximum T_B. Calculations for areas located around both centers are made for each satellite pass. Both will be presented.

The latent heat release (L. H. R.) over an area is given by

$$\text{L. H. R.} = L\rho \int_A R \, da, \qquad (1)$$

where ρ is the density of the rain (here assumed to be equal to 1.0 g cm^{-3}), L is the latent heat of condensation (2.5 x 10^{10} ergs g^{-1}), R is the rainfall rate, da is incremental area, and A is the area of integration. The rainfall rate R is determined from the microwave brightness temperature through the relation expressed in Fig. 1. The incremental area assigned to each rainfall rate point is a function of scan position. Although there is actually a slight overlap of adjacent ESMR scan spots, the assigned areas for the calculations are determined as if there is no overlap.

d. Sources of Error - The possible sources of error in the L. H. R. calculation area are: (1) instrumental error, (2) error in scan angle adjustment, (3) error in the selection of the freezing level height, (4) error in the derived T_B — rainfall rate relation, (5) error due to instrument resolution and (6) error produced by increased T_B due to surface roughness. The effect of random errors, such as instrument noise, is minimized because the calculations are integrations over a large number of points. Systematic errors, however, produce significant variations in the storm L.H.R. estimates.

Systematic instrument error is estimated to have a potential magnitude of 2 K, in terms of brightness temperature, T_B. Since the mean scan angle adjustment is only 2.5 K, a possible error in the adjustment of 1 K is assigned. For the freezing level selection, an inaccuracy of 4 K corresponding to a freezing level variation of 0.25 km is used. This is a reasonable freezing level error over the entire storm area considering the variation in freezing level from cloud cluster to mature storm referred to earlier. A potential difference of 5 K is arbitrarily used for the effect of the T_B - rain rate relationship.

The instrument resolution leads to a smaller than actual storm L.H.R. Heavy rain, with dimensions less than the resolution of the instrument, is underestimated. However, because the major rain features of tropical cyclones have dimensions approaching or greater than the instrument resolution, this effect is relatively small. Over the whole storm, this effect is estimated to be 4 K in terms of the brightness temperature, based partially on a calculation of the effect of still further smoothing of the data.

The effect of the enhanced contribution from a wind-driven sea is difficult to estimate. In areas of heavy rain the surface is, at least, partially masked by the rain. Since the highest wind speeds occur near the center of the mature storm where the rain is heaviest, the total effect of the increased surface contribution to the upwelling radiation is muted. A magnitude of 3 K is assumed for this effect. It tends to increase the L.H.R. estimate.

The last two effects (5 and 6) are of known, and opposite, sign and they approximately cancel each other out. The other four sources of error have estimated magnitudes of 2, 1, 4, and 5 K, respectively. The sign of the error is unknown in each case, but should be random. To evaluate the effect of these errors on the L.H.R. calculation, the following analysis is carried out. The error magnitudes (2, 1, 4, and 5 K) are potential values, or amplitudes. The actual systematic instrument error, for example, can be thought of as being normally distributed with a mean equal to zero and a standard deviation (σ) equal to 1.0. A value of σ equal to one-half of the error magnitude is reasonable, since the magnitude (2.0 for the instrument error) is equivalent to approximately one-half of the range. In a normal distribution, 95% of the values are within $\pm 2\ \sigma$; hence the error magnitudes are approximately equivalent to $2\ \sigma$.

The four error magnitudes thus convert into standard deviations (σ) of 1.0, 0.5, 2.0 and 2.5 K, respectively. The standard deviation of the combined errors is equal to the square root of the sum of squares, or 3.4 K. Therefore, the magnitude of the combined error, approximated by $2\ \sigma$, is 6.8 K.

A sample calculation made with temperatures 7 K lower than observed was made for the typhoon stage. The result shows a 25% difference in the L.H.R. over the storm. Thus the absolute magnitudes calculated in this study are estimated to be within about ± 25% of the actual L.H.R. Relative changes are probably much more accurately calculated.

4. Results

a. Storm Latent Heat Release - Tropical cyclone Nora formed in the last days of September 1973 at approximately 7°N, 138°E, 1200 km east of the Philippine Islands. It moved in a generally northwesterly direction, eventually becoming a very intense typhoon with maximum surface winds of 80 ms^{-1} and a minimum sea level pressure of 877 mb, one of the lowest on record. (Annual Typhoon Report, 1973). Satellite imagery of Nora (including microwave imagery) has been discussed by Allison et.al., (1974).

Calculations of the latent heat release were made at six times from 29 September to 5 October 1973. Nominally there would be about twice as many available observations. However, some potential observations were lost due to missing orbits and others were missed because usable data in adjacent orbital scans do not form a contiguous area and the storm was centered between data areas. During the period studied, the storm intensified from a weak tropical disturbance to a typhoon with maximum surface winds over 60 ms^{-1}. It then continued northwestward, crossing the Luzon Strait, and continuing to the China mainland. No additional, usable microwave passes were obtained of the storm.

The total latent heat release (L. H. R.) for a circular area of 4° latitude radius (~ 4 km) is given in Fig. 2 as a function of time. The solid line connects the points that result from calculations for the area centered on the subjectively determined axis of circulation. The X's denote results for the area centered on the point of maximum T_B, or maximum rainfall rate. A plot of the storm's maximum surface winds is also given.

The calculated L. H. R. ranges from 2.7 to 8.8 x 10^{21} ergs s^{-1}; this corresponds to a mean rain rate over the entire area of 0.6 to 2.0 mm hr^{-1}. The satellite-based value for the typhoon stage is compared to previous estimates in Table 1. Here all values have been converted to mean rainfall rate and given for circular areas of 1, 2, 3 and 4 degrees of latitude. Other than the present study, all estimates in the table are based on the moisture budget technique. There is only partial agreement between the estimates. Within 1° latitude, the satellite-based estimate agrees with one study, but is only one half as large as the other estimates. The three estimates at 2° latitude are in good agreement. The variability in Table 1 is probably a result of both the different techniques and also the natural variability of the phenomenon.

Latent heat release calculations have also been made using numerical models of mature hurricanes. A value of 4.7 x 10^{21} ergs sec^{-1} was computed

Table 1
Mean Rain Rate Comparisons for Mature Storms. Units: mm hr^{-1}

	Radius of Area Covered			
	1°lat.	2°lat.	3°lat.	4°lat.
Present Study (Nora, 1972)	6.8	5.2	3.1	2.0
Hughes (1952) (Composite)	14.0	4.5	2.1	1.2
Palmen and Riehl (1957) (Composite)	—	5.2	—	—
Riehl and Malkus (1961) (Daisy, 1958)	13.6	—	—	—
Miller (1962) (Helene, 1958)	13.9	—	—	—
Hawkins and Rubsam (1968) (Hilda, 1964)	6.3	—	—	—

by Kurihara (1975) for a radius of 500 km using an axisymmetric model. Tuleya and Kurihara (1975) calculated 5.8×10^{21} ergs sec^{-1} (for 500 km radius) for the latent heat release simulated by a three dimensional model. Anthes (1972) calculated a magnitude of 12.6×10^{21} ergs sec^{-1} for the domain of an asymmetric hurricane. These values are comparable to the 8.8×10^{21} ergs s^{-1} of this study for a mature storm.

The most striking feature of the L. H. R. in Fig. 2 is the continuous increase with time. As the system develops from a disturbance on 29-30 September to a depression (1-2 October), there is an increase of 50% in the L. H. R. This increase in L. H. R. over a limited area is consistent with the idea of tropical cyclogenesis. If this increase during the formative stages is duplicated in other cases, a basis would exist for monitoring tropical disturbances with this type of data.

The estimated L. H. R. during the depression stage is 4×10^{21} ergs s^{-1}. As the cyclone continues to intensify, the L. H. R. also rises from approximately 4 to 7×10^{21} ergs s^{-1} during the storm phase, and to above that as it becomes a typhoon with a calculated maximum of 8.8×10^{21} ergs s^{-1}. An increase in L.H.R. as a tropical cyclone goes from storm stage to hurricane is also indirectly noted by Riehl and Malkus (1961) for hurricane Daisy of 1958. Horizontal latent heat flux was calculated at two times, once when the storm was not quite a hurricane and again when it was a mature hurricane with mid-tropospheric winds of about 60 ms^{-1} and a central pressure of 950 mb. At a radius of 1° latitude, the inward flux went up by more than a factor of 2.5 between the two times. This would result in a similar increase in the L. H. R. inside the circle. For the present case, the L. H. R. inside the 1° latitude circle also rose, by a factor greater than 2, between the 3 October and the 5 October observation. These relationships indicate a possible application of microwave data in helping to determine the intensity and intensity changes of tropical cyclones.

The L. H. R. within 4° latitude can be thought of as being proportional to the product of the area covered by precipitation and the mean precipitation rate in that precipitation area. These two parameters are displayed in Figs. 3 and 4, respectively. The latent heat release per unit area of precipitation in Fig. 4 is proportional to the mean rain rate. The precipitation area (Fig. 3) generally increases throughout the period, going from fractional area coverage of 0.3 to 0.8. These are probably overestimates of rain coverage due to the coarse resolution of the data. The L. H. R./area (Fig. 4) shows no systematic increase until the cyclone goes from depression to storm and typhoon stage. These two diagrams indicate that as the L. H. R. increases in the early stages (29 September - 1 October), the intensity of the precipitation does not increase sharply, but the area of rain expands. As further intensification occurs (1 October - 5 October), both the area of rain increases and the mean rain rate in that area rises.

b. Radial Distribution of Rainfall - Tne mean rainfall rate as a function of distance from the subjectively determined circulation centers is shown in Fig. 5 for the last four observations, occurring as the system deepened. For the disturbance and depression observations, the maximum rainfall ring is located at 100-175 km with a magnitude of just over 2 mm hr^{-1}. The 3 October storm stage observation indicates that the ring of maximum rainfall has not moved significantly inward, but has increased in magnitude to about 5 mm hr^{-1}. After that, the rainfall concentrates toward the center with a large increase occurring within 100 km. Although the "eye" of a storm can sometimes be found in the microwave data, the coarse resolution does not always show a decrease in precipitation at the center of intense storms.

The concentration of rainfall toward the center of circulation is better shown in Fig. 6, which displays the cumulative percentage of rainfall or L.H.R., integrating from the center outward to 250 km. At 100 km, the percentages are 12, 16, and 24% for the three observations as the storm intensifies.

This centerward concentration of precipitation agrees with model results such as Rosenthal (1970) and Kurihara (1975). They both indicate that in their axisymmetric hurricane models the ring of maximum upward velocity moves inward as the circulation intensifies.

c. Rainfall Intensity - This section deals with determining what are the relative contributions of various rainfall intensities to the total volume precipitation or L. H. R. in the storm. Fig. 7 shows the distribution of volume rain rate per unit rain rate (units in terms of area) as a function of rain rate itself for the first four observations of the area centered on the maximum T_B. The area under the curve is the volume rain rate in the storm, which is proportional to the L. H. R. The distribution in Fig. 7 for the three disturbance observations and the one depression observation all indicate that the peak contribution is in the 1-4 mm hr^{-1} range with the contribution falling off rapidly with increasing rain rate.

Fig. 8 shows similar curves for the storm and typhoon stage along with the disturbance and depression stage. Unlike those in Fig. 7, the curves in Fig. 8 are the result of calculations over the area centered on the circulation axis. The two observations for 1 and 2 October on both figures are very similar, indicating that the results are not sensitive to slight shifts in the location of the area. The area positioned on the storm center is preferable for the latter stages of the storm.

The storm stage and typhoon distributions in Fig. 8 are considerably different from when the circulation was weaker. Not only have the areas under the curves grown, indicating rising L. H. R., but the relative contributions have changed. As the storm intensifies from depression to typhoon, the larger rain rates increase their relative contribution. This can be seen clearly in Fig. 9, which shows the cumulative percentage contribution of rainfall intensity at the four times. While during the disturbance and depression stages the contribution of rain rates ≥ 6 mm hr^{-1} was 8% and 14%, the later observations indicate values of 30% and 38% for the storm and typhoon stages. Thus as the storm intensifies, larger rain rates become increasingly more important.

5. Conclusions

Data from a satellite passive microwave radiometer have been shown to be useful to study quantitatively the rainfall characteristics of tropical cyclones, and are potentially useful in the monitoring of tropical cyclone intensity. The calculations for this particular case indicate that the latent heat release (L.H.R.) of the storm rises as the intensity of the circulation increases. Even before the depression stage was reached, the L. H. R. increased from less than 3×10^{21} ergs s^{-1} to about 4×10^{21} ergs s^{-1}. From depression to typhoon, the L. H. R. grows from 4 to nearly 9×10^{21} ergs s^{-1}. The increase in L. H. R. in the early stages is shown to be associated with an expansion of the rain area, while the intensity of the rainfall remains relatively steady. From depression to typhoon, however, both the area and intensity of the rainfall increase.

As the cyclone deepens, the rainfall is observed to concentrate toward the center of the storm. In addition, higher rainfall rates make an increasingly larger relative contribution to the storm L. H. R. during this period.

REFERENCES

Allison, L. J., E. B. Rodgers, T. T. Wilheit and R. W. Fett, 1974: Tropical cyclone rainfall as measured by the Nimbus 5 Electrically Scanning Microwave Radiometer. Bull. Amer. Meteor. Soc., 55, 1074-1089.

Anthes, R. A., 1972: Development of asymmetries in a three-dimensional numerical model of the tropical cyclone. Mon. Wea. Rev., 100, 461-476.

Charney, J. G. and A. Eliassen, 1964: On the growth of the hurricane depression. J. Atmos. Sci., 21, 68-75.

Hawkins, H. F. and D. Rubsam, 1968: Hurricane Hilda, 1964: Part II. Mon. Wea. Rev., 96, 617-636.

Hughes, L. A., 1952: On the low-level wind structure of tropical storms. J. Met., 9, 422-428.

Kidder, S. Q., 1976: Tropical oceanic precipitation frequency from Nimbus 5 microwave data. Atmospheric Science Paper No. 248, Colorado State University, 49 pp.

Kurihara, Y., 1975: Budget analysis of a tropical cyclone simulated in an axisymmetric numerical model. J. Atmos. Sci., 32, 25-59.

Miller, B. I., 1962: On the momentum and energy balance of hurricane Helene (1958). National Hurricane Research Project Report No. 53, 19 pp.

Palmen, E., and C. W. Newton, 1969: Atmospheric Circulation Systems. Academic Press, New York, 381-383 and 481.

_____ and H. Riehl, 1957: Budget of angular momentum and energy in tropical cyclones. J. Meteor., 14, 150-159.

Riehl, H. and J. Malkus, 1961: Some aspects of Hurricane Daisy, 1958. Tellus, 13, 181-213.

Rosenthal, S. L., 1970: A circularly symmetric primitive equation model of tropical cyclone development containing an explicit water vapor cycle. Mon. Wea. Rev., 98, 643-663.

Tuleya, R. E. and Y. Kurihara, 1975: The energy and angular momentum budgets of a three-dimensional tropical cyclone model. J. Atmos. Sci., 32, 287-301.

U. S. Fleet Weather Center/Joint Typhoon Warning Center, 1973 Annual typhoon report. Guam, Mariana Is., 99 pp.

Wilheit, T. T., 1972: The electrically scanning microwave radiometer (ESMR) experiment. Nimbus 5 Users Guide, NASA Goddard Space Flight Center, 55-105.

_____, M. S. V. Rao, T. C. Chang, E. B. Rodgers and J. S. Theon, 1975: A satellite technique for quantitatively mapping rainfall rates over the oceans. NASA X-911-75-72, Goddard Space Flight Center, 28 pp.

_____, J. S. Theon, W. E. Shenk, L. J. Allison and E. B. Rodgers, 1976: Meteorological interpretations of the images from the Nimbus 5 Electrically Scanned Microwave Radiometer, J. Appl. Met., 15, 166-172.

Williams, K. T. and W. M. Gray, 1973: Statistical analysis of satellite-observed trade wind clusters in the western North Pacific. Tellus, 25, 313-336.

Yanai, M., 1975: U.S. quadrennial report to IUGG: tropical meteorology. Tropical Meteorology Paper No. 8, Department of Meteorology, University of California, Los Angeles, p 81.

FIGURE CAPTIONS

1. Rainfall rate as a function of Nimbus 5 ESMR brightness temperature, T_B for a freezing level of 5 km.

2. Latent heat release (L. H. R.) as a function of time for tropical cyclone Nora from 29 September to 5 October 1973. Calculations are for a circular area of radius 4° latitude. Data connected by the solid line are for the area surrounding the center of circulation; X's are results for areas centered on maximum brightness temperature. The storm's maximum surface winds are also plotted. (Dashed Line)

3. Precipitation area as a function of time. Dots and X's denote calculations for areas centered on the axis of circulation and maximum T_B, respectively.

4. Latent heat release (L. H. R.) per unit area as a function of time. Dots and X's denote calculations for areas centered on the axis of circulation and maximum T_B, respectively.

5. Mean rainfall rate as a function of radial distance from the storm center for four observations as the storm intensified.

6. Cumulative percentage of total rainfall as a function of radial distance from the storm center to 250 km for three observations.

7. Contribution of various rain rate magnitudes to total volume precipitation in early stages of storm.

8. Contribution of various rain rate magnitudes to total volume precipitation as storm intensifies.

9. Cumulative percentage contribution to total storm rainfall of rain rates at and above particular values.

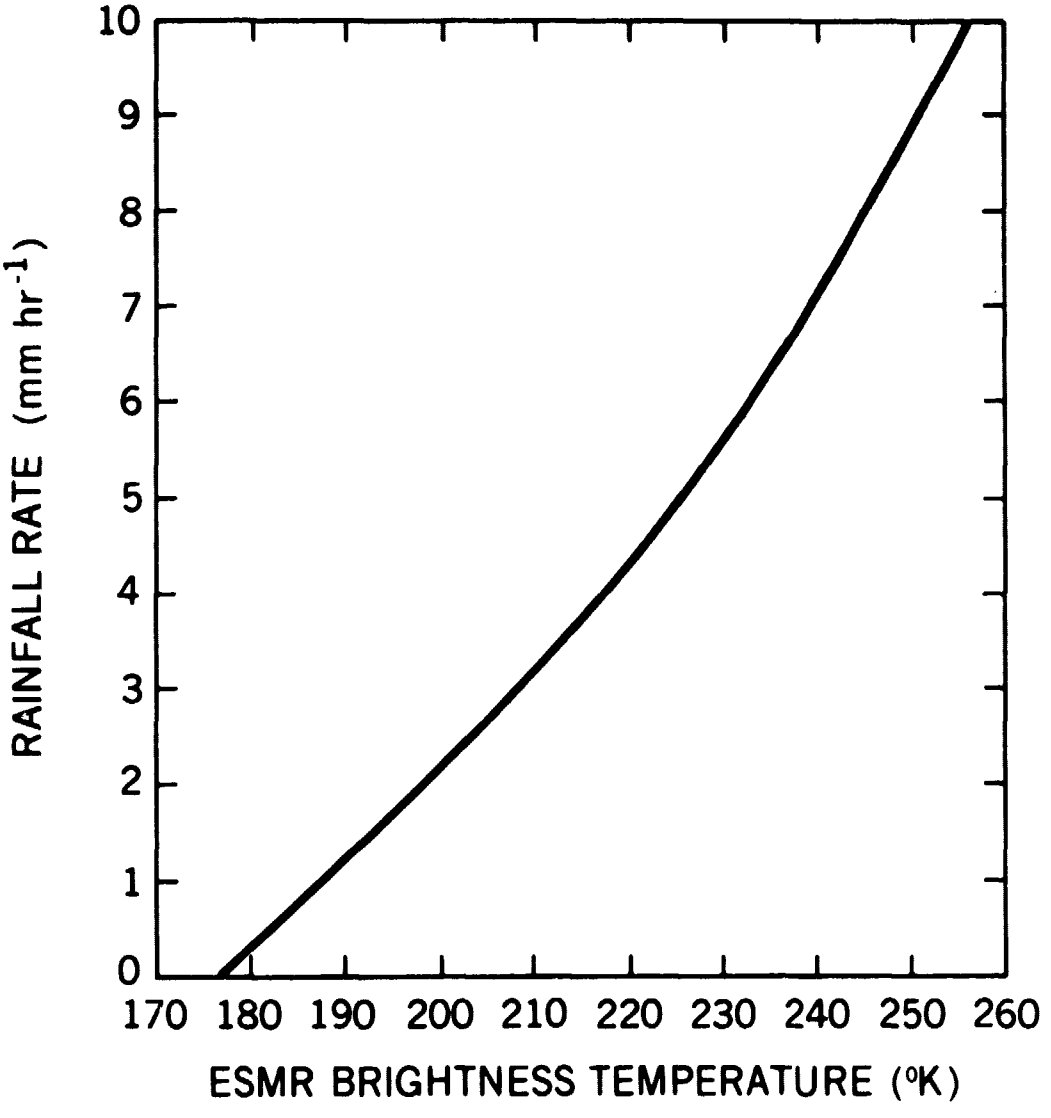

Fig. 1 Rainfall rate as a function of Nimbus 5 ESMR brightness temperature, T_B for a freezing level of 5 km

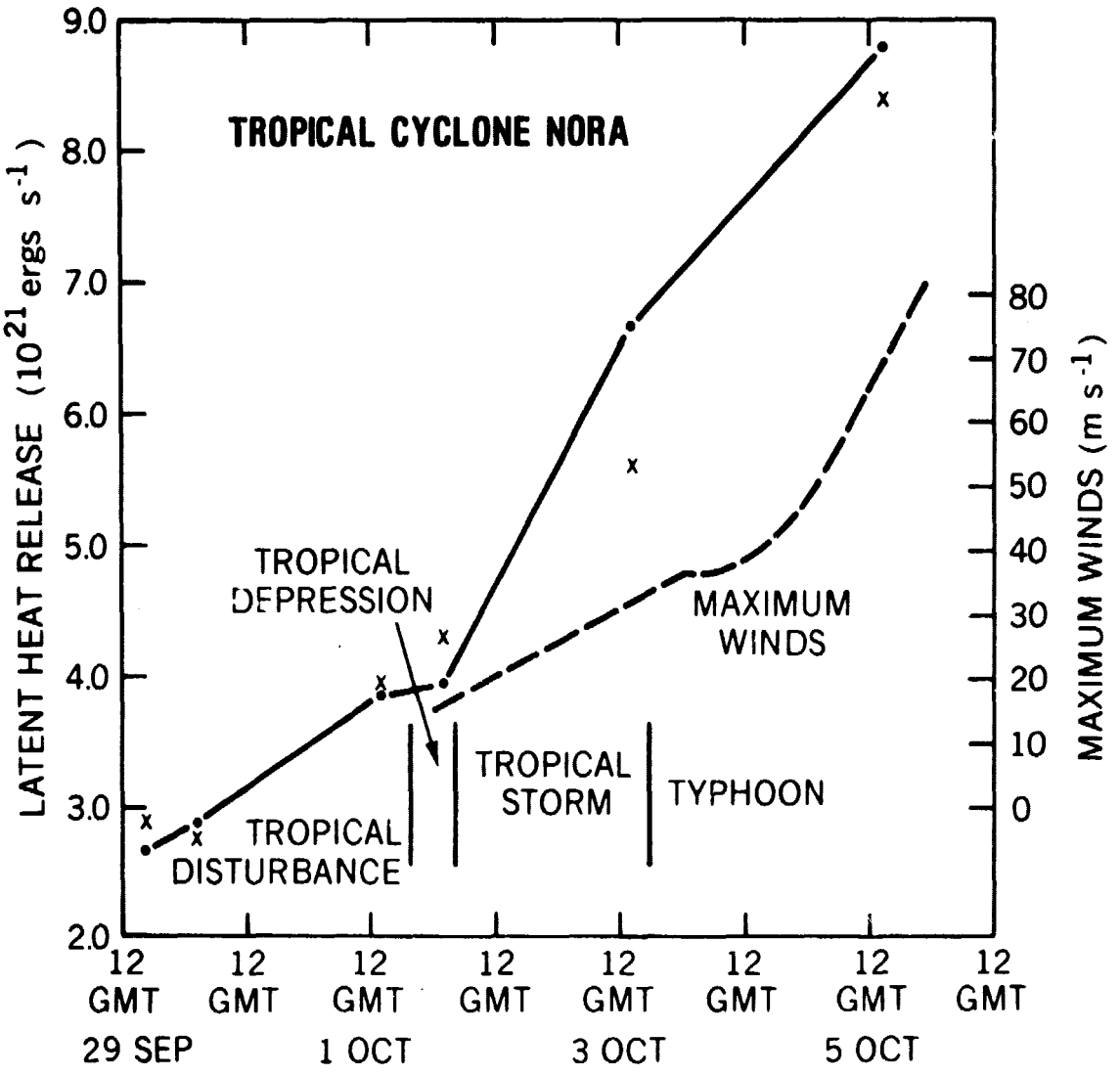

Fig. 2 Latent heat release (L. H. R.) as a function of time for tropical cyclone Nora from 29 September to 5 October 1973. Calculations are for a circular area of radius 4 latitude. Data connected by the solid line are for areas surrounding the center of circulation; X's are results for areas centered on maximum brightness temperature. The storm's maximum surface winds are also plotted (Dashed Line).

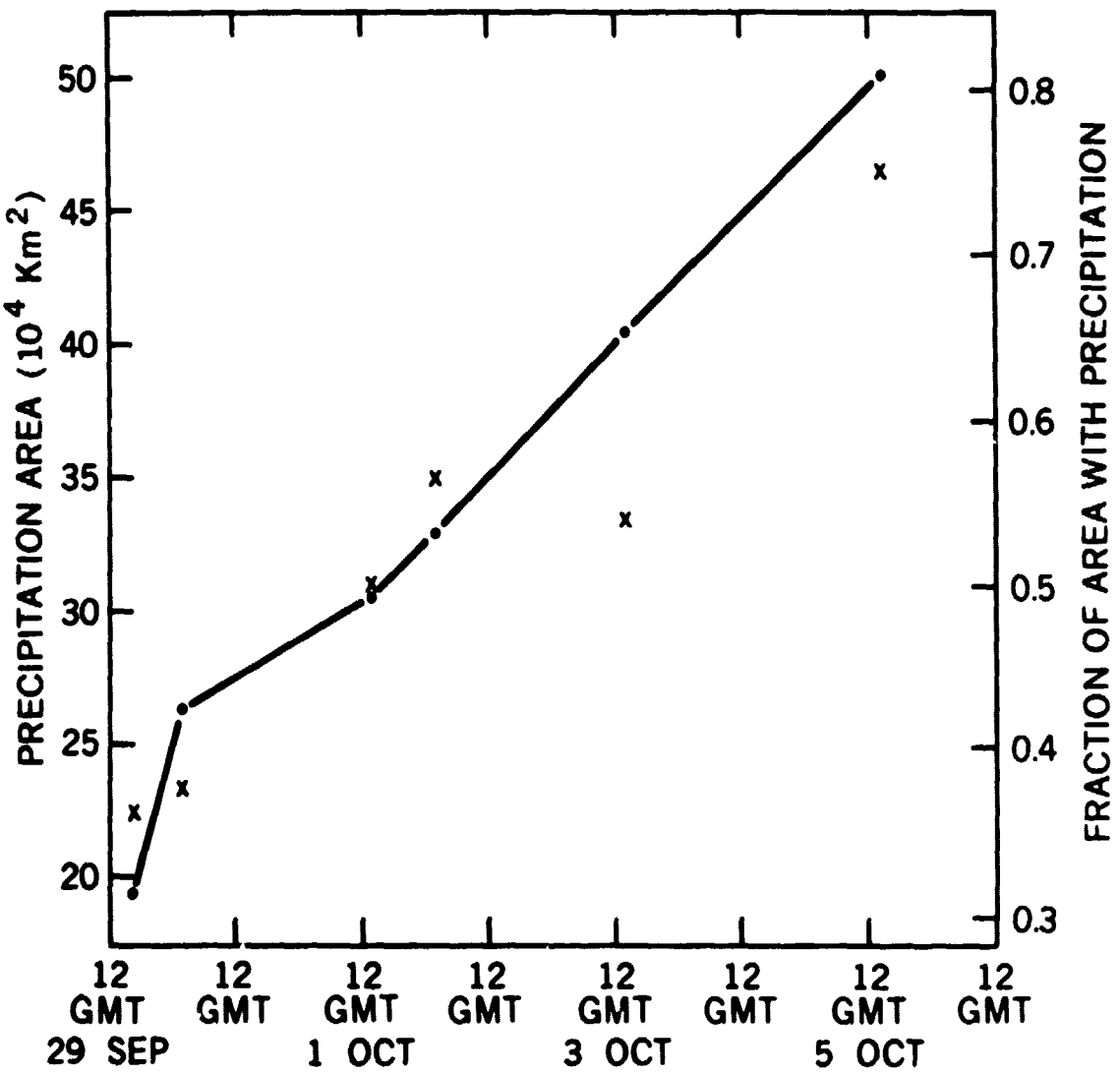

Fig. 3 Precipitation area as a function of time. Dots and X's denote calculations for areas centered on the axis of circulation and maximum T_B, respectively

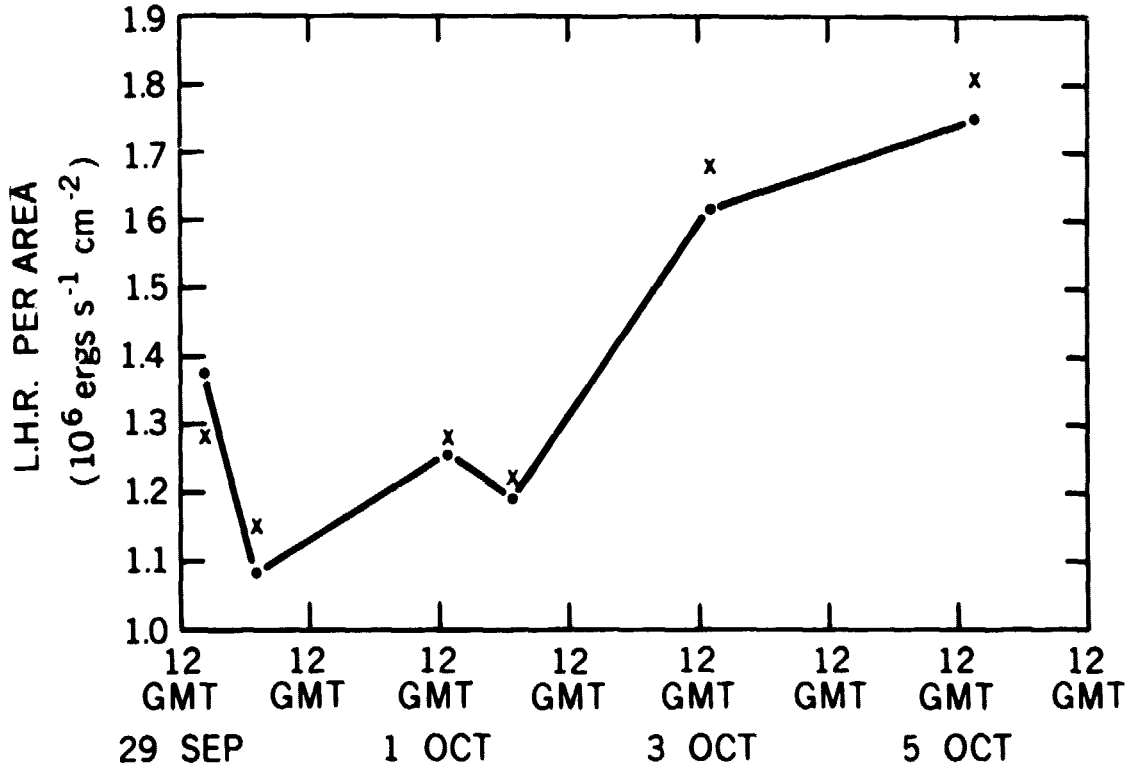

Fig. 4 Latent heat release (L. H. R.) per unit area as a function of time. Dots and X's denote calculations for areas centered on the axis of circulation and maximum T_B, respectively

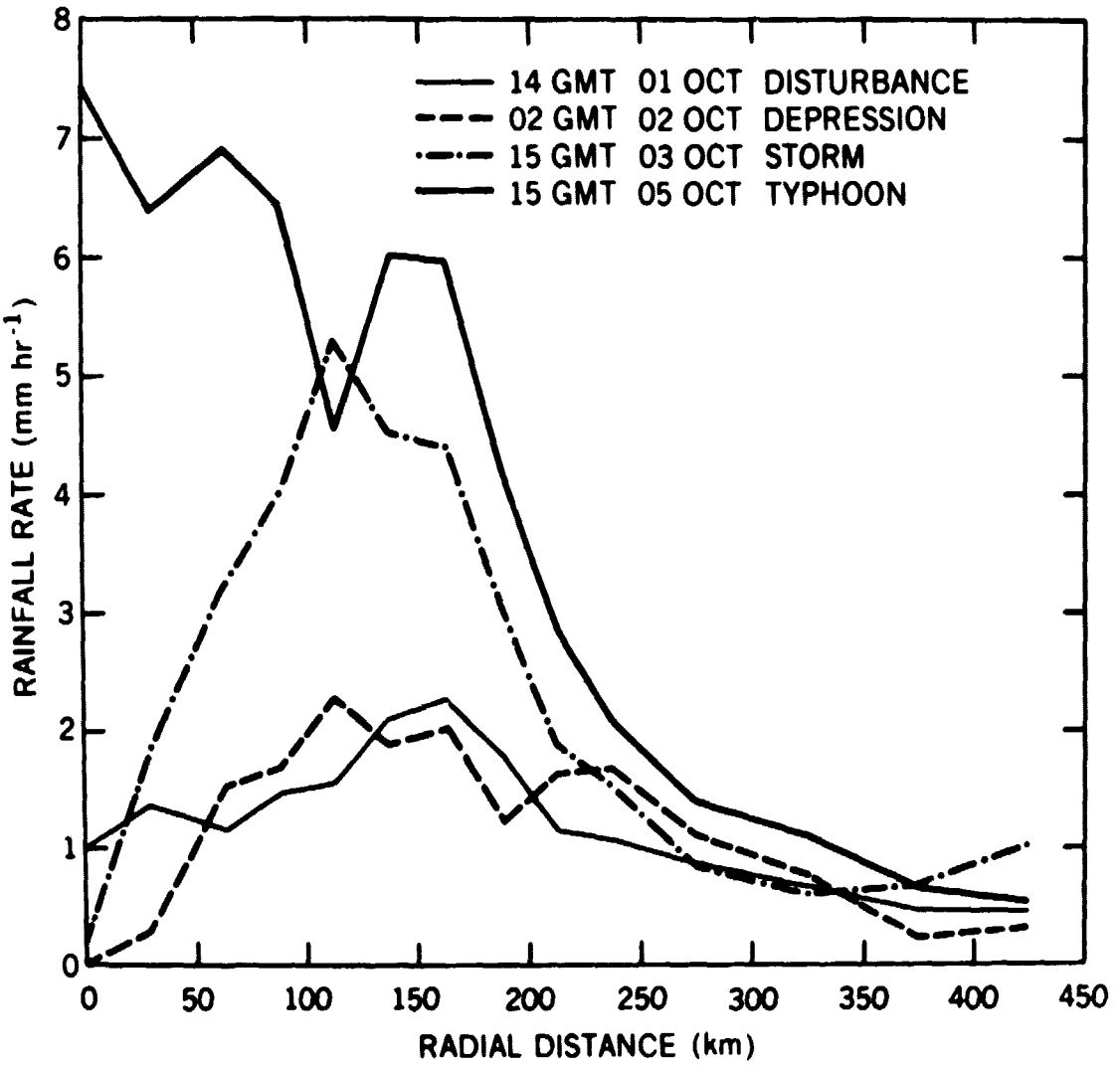

Fig. 5 Mean rainfall rate as a function of radial distance from the storm center for four observations as the storm intensified

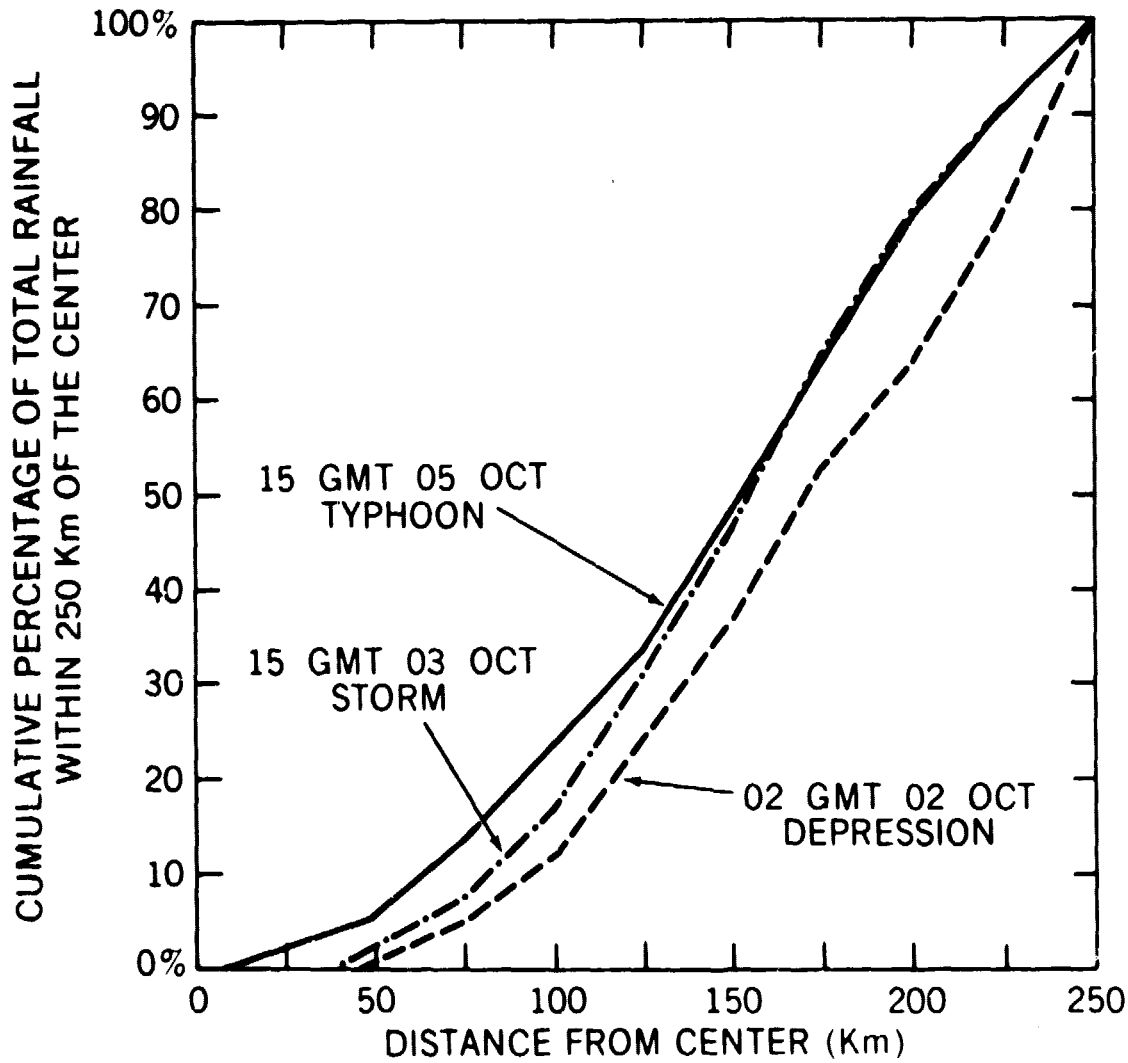

Fig. 6 Cumulative percentage of total rainfall as a function of radial distance from the storm center to 250 km for three observations

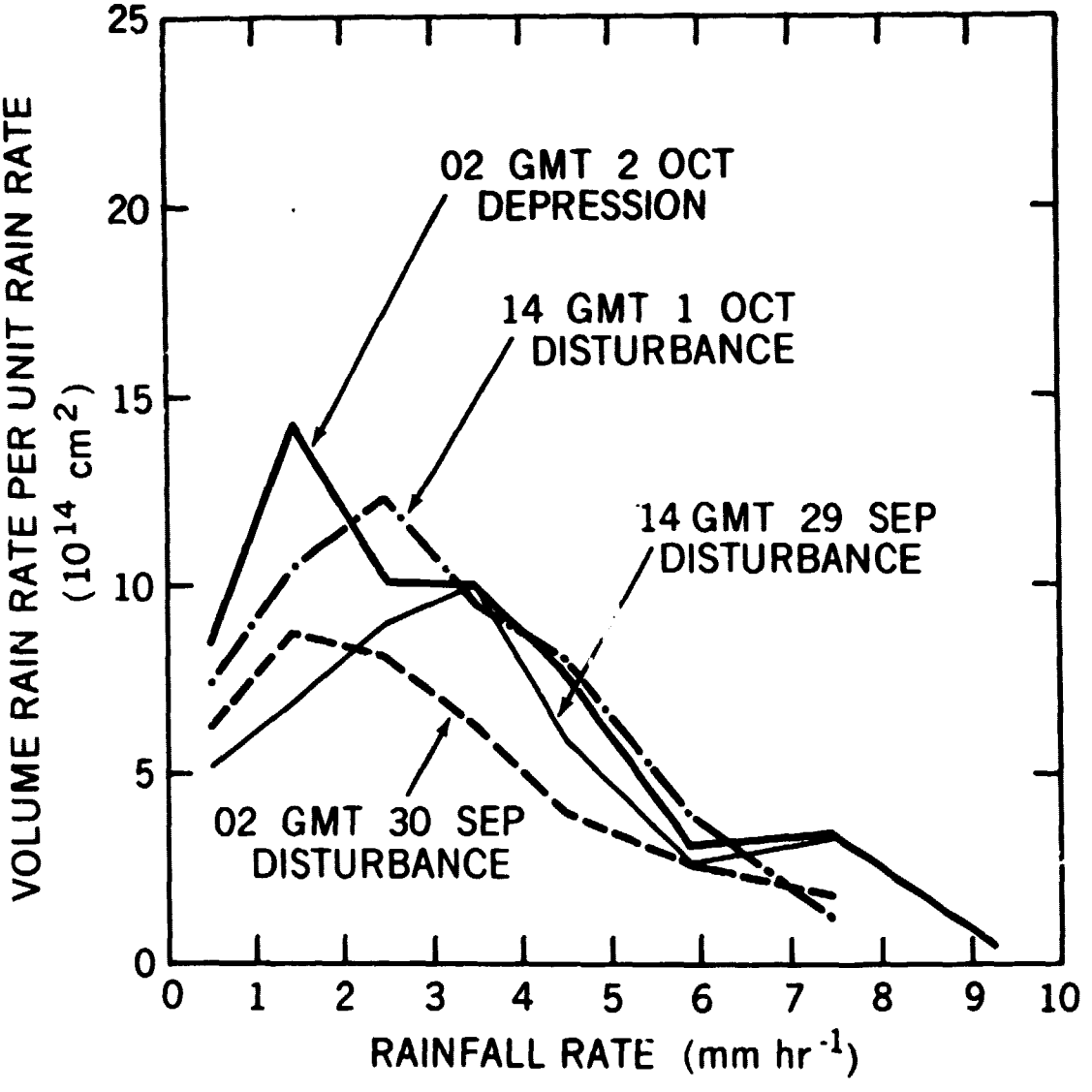

Fig. 7 Contribution of various rain rate magnitudes to total volume precipitation in early stages of storm

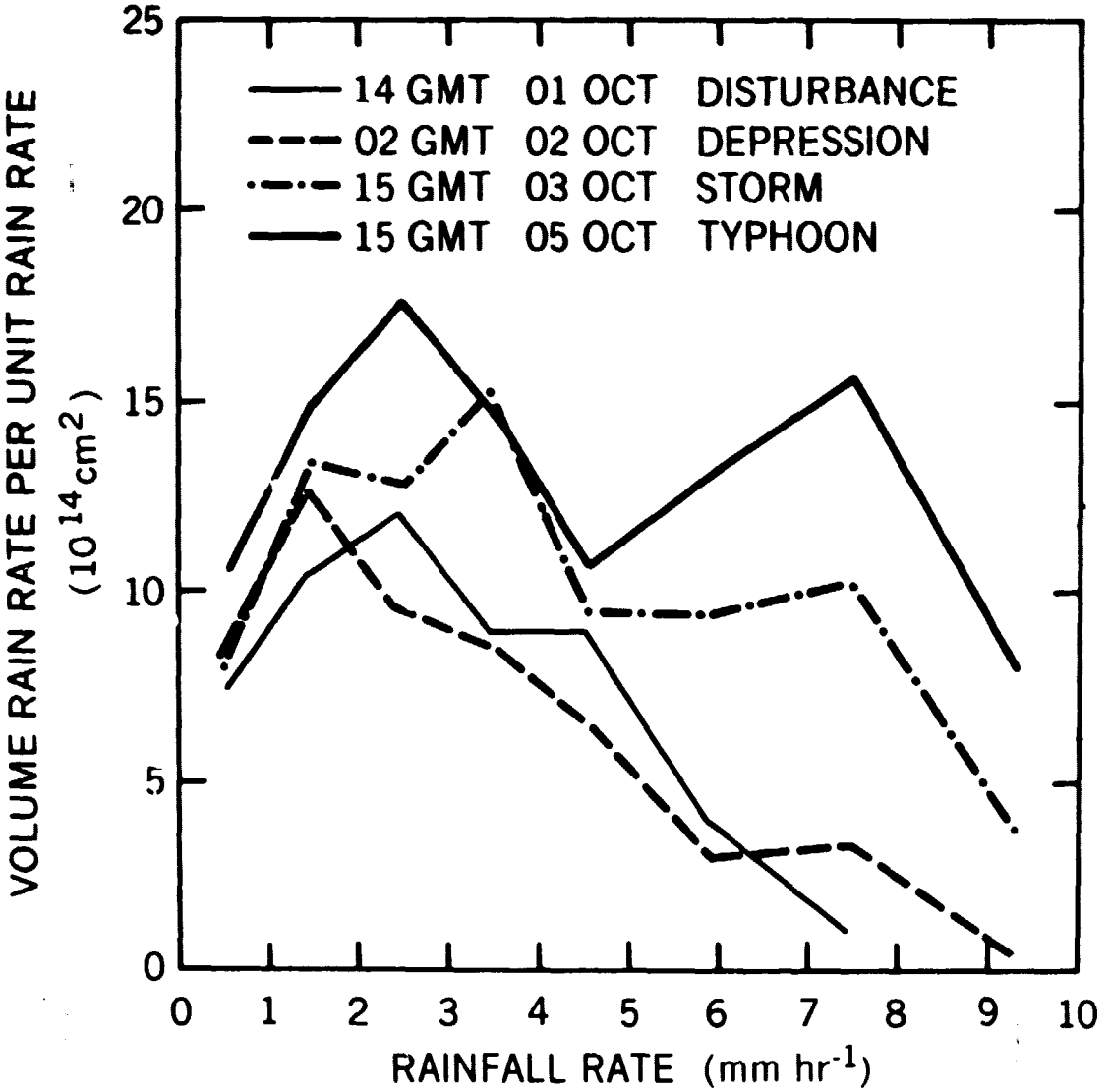

Fig. 8 Contribution of various rain rate magnitudes to total volume precipitation as storm intensifies

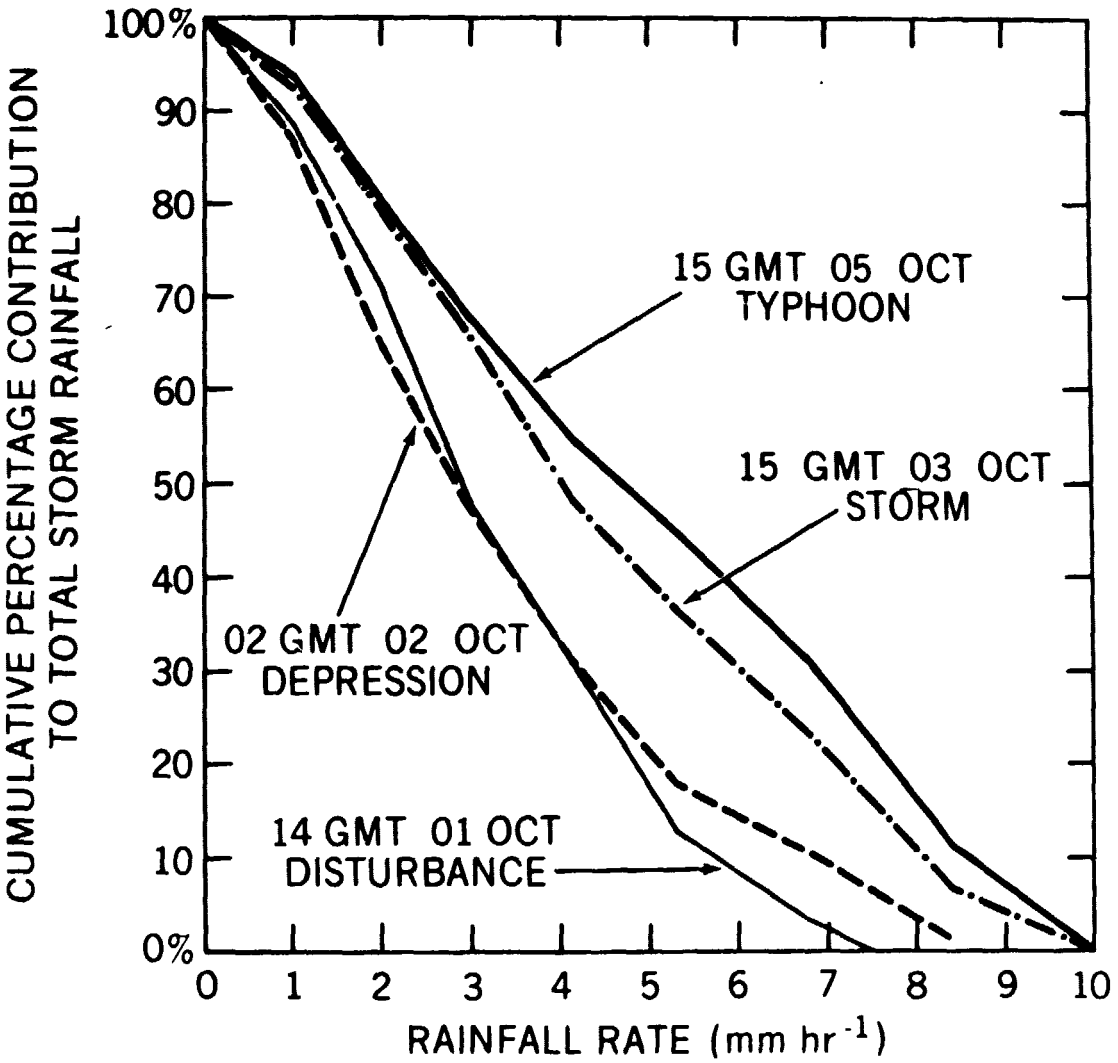

Fig. 9 Cumulative percentage contribution to total storm rainfall of rain rates at and above particular values